AD-A123 995 BONDABILITY OF TI ADHERENDS III OXIDE STABILITY AND SUBSTRATE CORROSION(U) MARTIN MARIETTA LABS BALTIMORE MD M NATAN ET AL. SEP 82 MML-TR-82-20C 1/1

UNCLASSIFIED N00019-81-C-0355 F/G 11/1 NL

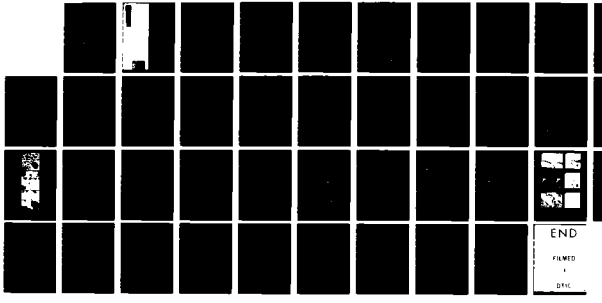

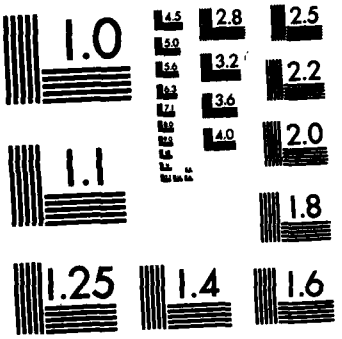

MARTIN MARIETTA

Martin Marietta Laboratories

(6)

MML TR 82-20c

BONDABILITY OF Ti ADHERENDS

III. OXIDE STABILITY AND SUBSTRATE CORROSION

September 1982

Final Report for Period
August 15, 1981 through August 15, 1982

Prepared by:

Menachem Natan
John D. Venables
Martin Marietta Laboratories
1450 South Rolling Road
Baltimore, Maryland 21227

Prepared for:

Department of the Navy
Naval Air Systems Command
Washington, D.C. 20361

Under Contract No. N00019-81-C-0355

Baltimore DCAS Management Area
300 East Joppa Road, Room 200
Towson, Maryland 21204
ATTN: Mr. William L. Sunday, ACO

SECURITY CLASSIFICATION OF THIS PAGE (When Data Entered)

REPORT DOCUMENTATION PAGE

READ INSTRUCTIONS BEFORE COMPLETING FORM

1. REPORT NUMBER	2. GOVT ACCESSION NO. AD-A123995
3. RECIPIENT'S CATALOG NUMBER	
4. TITLE (and Subtitle) Bondability of Ti Adherends	5. TYPE OF REPORT & PERIOD COVERED Final report (3rd year) Aug. 15, 1981 - Aug. 15, 1982
	6. PERFORMING ORG. REPORT NUMBER MML TR 82-20c
7. AUTHOR(s) Menachem Natan, John D. Venables	8. CONTRACT OR GRANT NUMBER(s) N00019-81-C-0355
9. PERFORMING ORGANIZATION NAME AND ADDRESS Martin Marietta Laboratories, 1450 S. Rolling Road, Baltimore, Maryland 21227	10. PROGRAM ELEMENT, PROJECT, TASK AREA & WORK UNIT NUMBERS
11. CONTROLLING OFFICE NAME AND ADDRESS Department of the Navy, Naval Air Systems Command, Code: AIR-5163C2, Washington, D.C. 20361	12. REPORT DATE September 1982
	13. NUMBER OF PAGES 38
14. MONITORING AGENCY NAME & ADDRESS(if different from Controlling Office) Baltimore DCAS Management Area, 300 E. Joppa Road, Room #200, Towson, Maryland 21204, ATTN: Mr. William L. Sunday, ACO	15. SECURITY CLASS. (of this report) UNCLASSIFIED
	15a. DECLASSIFICATION/DOWNGRADING SCHEDULE

16. DISTRIBUTION STATEMENT (of this Report)

Approved for public release; distribution unlimited.

17. DISTRIBUTION STATEMENT (of the abstract entered in Block 20, if different from Report)

N/A

18. SUPPLEMENTARY NOTES

19. KEY WORDS (Continue on reverse side if necessary and identify by block number)

Titanium adhesive bonding, titanium oxide stability, corrosion, AES, electron microscopy.

20. ABSTRACT (Continue on reverse side if necessary and identify by block number)

As the last part of a three-year program designed to evaluate surface pretreatments of titanium for adhesive bonding, this study concentrated on the effect of oxide stability on bond durability. We found that if the oxide is amorphous and highly defective, it will be susceptible to morphological and structural changes. The bond to epoxy, which probably involves only the uppermost atomic layer of the oxide, may be disrupted by surface migration and crystallization in the oxide and by processes leading to the base metal corrosion in water. These mechanisms are

DD FORM 1 JAN 73 1473

SECURITY CLASSIFICATION OF THIS PAGE (When Data Entered)

20. known to be highly temperature sensitive and are probably accelerated in the presence of water. The use of Auger electron spectroscopy and sputter profiling for studying oxide transformations is also illustrated.

MML TR 82-20c

BONDABILITY OF Ti ADHERENDS

III. OXIDE STABILITY AND SUBSTRATE CORROSION

Final Report for Period

August 15, 1981 through August 15, 1982

September 1982

Prepared for:

Department of the Navy
Naval Air Systems Command
Washington, D.C. 20361

Under Contract No. N00019-81-C-0355

Prepared by:

Menachem Natan
John D. Venables
Martin Marietta Laboratories
1450 South Rolling Road
Baltimore, Maryland 21227

M. Natan
Principal Investigator

TABLE OF CONTENTS

LIST OF FIGURES

FIGURES (continued)

I. INTRODUCTION

Oxide films on titanium alloys play a very important role in determining the mechanical properties of adhesive bonds used for joining metal-to-metal or metal-to-composite structures in the aircraft industry. Depending on the surface preparation technique, these films range in thickness from tens to thousands of angstroms, and exhibit wide variations in oxide morphology.[1-10] For instance, it has been shown that anodization in a chromic acid bath creates a thick, porous oxide film having excellent bonding properties.[1-3] However, exposure to pure water in the temperature range 70-100°C causes changes in the film that allow corrosion of the titanium substrate.[4] The destabilization of the film will likely contribute to a decrease in the durability of an

---

1 B.M. Ditchek, K.R. Breen, T.S. Sun, J.D. Venables, and S.R. Brown, in Proc. 12th Natl. SAMPE Tech. Conf. (Seattle, WA, 1980), p. 882.
2 B.M. Ditchek, K.R. Breen, T.S. Sun and J.D. Venables, in Proc. 25th Natl. SAMPE Symp. (San Diego, CA, 1980), p. 13.
3 M. Natan, J.D. Venables, and K.R. Breen, in Proc. 27th Natl. SAMPE Symp. (San Diego, CA, 1982), p. 178.
4 M. Natan and J.D. Venables, submitted to J. of Adhesion.
5 A.A. Roche, J.S. Solomon, and W.L. Baun, Appl. Surf. Sci. 7, 83, (1981).
6 J.M. Abd El Kader, F.M. Abd El Kader, H.A. El Shayeb, and M.G.A. Khedr, Br. Corros. J. 16, 111 (1981).
7 F. Dalard, C. Montella, and J. Gandon, Surf. Technol. 8, 203 (1979).
8 G. Blondeau, M. Froelicher, M. Forment, and A. Hugot-LeGoff, in Proc. 7th Int. Vac. Congr. and 3rd Int. Conf. Solid Surf. (Vienna, 1977), p. 1789.
9 K.W. Allen, H.S. Alsalim, and W.C. Wake, J. Adhes. 6, 153 (1974).
10 A. Polity, G. Jouve, and P. Lacombe, J. Less-Com. Met. 56, 263 (1977).

adhesive bond between oxide and epoxy, as has already been shown for Al,[11] and is therefore of great concern.

The original purpose of this study, which covers the third year of a three-year period, was to concentrate on the characterization of Ti-to-graphite epoxy bonds. However, as we progressed it became apparent that it was more important to understand the process of Ti surface changes in moist environments. We therefore decided to limit the study to pre-treated Ti-surfaces and focus on oxide transformations and substrate corrosion. These were studied with electron microscopy (SEM and TEM) and Auger electron spectroscopy (AES). Various topics are presented as follows:

Section II is a description of the experimental tools and techniques used in the study.

Section III deals with the nature of the anodic film on a Ti-6Al-4V alloy. It emphasizes the novel use of an advanced surface technique, Auger electron spectroscopy (AES), to differentiate between amorphous and crystalline structures. We show that amorphous Ti oxides are inherently less stable than crystalline ones, and more likely to have atomic defects such as oxygen vacancies in addition to gross non-stoichiometry. Defects may aid structural changes in the oxide upon heating and exposure to humid environments and lead to debonding between the top oxide atomic layer and the epoxy. The AES method described provides some evidence for the higher instability and greater disorder of the amorphous oxides.

---

11 J.D. Venables, D.K. McNamara, J.M. Chen, B.M. Ditchek, T.I. Morgenthaler, and T.S. Sun. in Proc. 12th National SAMPE Conf. (Seattle, WA, 1980), p. 909.

The immersion studies performed on (chromic acid) anodized coupons are described in Section IV. Structural and morphological changes occuring after immersion were investigated by electron microscopy and some chemical information was obtained with AES. Also described is a method for studying the corrosion of anodized Ti surfaces using AES and sputter profiling. Preliminary results on the kinetics of the corrosion process obtained with this method are presented.

Section V is a discussion of the results and an update of a tentative transformation model (proposed in a previous report) for water-immersed amorphous anodized films, with implications relevant to adhesive bond durability. It concludes with suggestions for future studies, especially in the areas of structural changes (electron microscopy) and corrosion kinetics.

Although this work is a continuation of a comprehensive evaluation of approximately ten surface pretreatments on titanium, the decision to concentrate on the 10V-chromic acid anodization (CAA) process is not arbitrary. It has been shown[12] that this treatment provides the best durability and that there is a marked similarity between changes observed in the CAA oxide and other surfaces that contain amorphous oxides (e.g., after TURCO (TU), phosphate fluoride (PF), alkaline peroxide (AP), and Pasa Jell (LP) treatments). We therefore suggest that the results obtained on the CAA surface are relevant to surfaces prepared by other pretreatments, provided they acquire amorphous oxides.

---

[12] M. Natan, K.R. Breen, and J.D. Venables, MML TR 81-42(c), Martin Marietta Laboratories, Baltimore, MD, Report to Navairsyscom, September 1981.

II. EXPERIMENTAL

Ti-oxide films were formed in two ways: 1) by anodization in a chromic acid bath, or 2) by reactive sputtering deposition in vacuum. Bulk oxides used as calibration standards either were purchased as powders or were prepared in the laboratory.

A. ANODIZATION

Ti-6Al-4V coupons (50-μm-thick sheet) were degreased in trichloroethylene vapor for 10 minutes and pickled in a solution containin 15 vol.% 70% HNO_3 and 3 vol.% 50% HF for 30 seconds. After a 2-minute rinse in distilled water, each coupon was anodized in an electrolyte, consisting of 5% chromic acid and 1 g/l NH_4F, at 10V for 20 minutes. The anodized coupons received two 2-minute rinses in distilled water and were dried for 2 to 5 minutes in a hot air flow. Specimens with surface areas of approximately 1 cm^2 were sheared from the coupon. The bare edges lacked an anodic film, but probably were instantly covered with a natural oxide layer. To demonstrate that edge effects did not significantly influence the behavior, some water immersion tests were repeated on totally anodized coupons with identical results.

B. REACTIVE SPUTTER DEPOSITION (RSD)

Reactive sputter deposition (RSD) was performed in a Technics ion-miller vacuum chamber, in a 50% Ar, 50% O_2 atmosphere at 4×10^{-4} torr (5×10^{-2} Pa). The sputtered target was pure Ti foil, and oxide films were deposited on Ti, pure Al, and glass substrates. Thickness was monitored with a quartz crystal. The Al substrate was ion milled to a thin foil, and the crystal structure of the film was determined by electron diffraction.

C. Ti-OXIDE STANDARDS

"Amorphous" TiO_2 was prepared in the laboratory by reacting $TiCl_4$ with NH_4OH and drying the precipitate at low temperature. X-ray diffraction (XRD) analysis of the powder revealed the presence of very broad peaks corresponding to anatase crystallites 50-100 Å in diameter. The sample was ground to fine powder prior to the AES measurements. In addition, crystalline TiO, Ti_2O_3, and TiO_2 powders were purchased from CERAC, Inc. Purity, particle size, and crystal structure are shown in Table I.

TABLE I

OXIDE STANDARDS USED IN STUDY

Material	Purity (%)	Particle (mesh)	Crystal Structure (based on X-ray diffraction analysis)
TiO	99.9	-325	monoclinic PDF-1078
Ti_2O_3	99.8	-325	hexagonal PDF 10-63
TiO_2	99.9	-325	anatase PDF 21-1272
TiO_2	99.995	-100	rutile PDF 21-1276

D. AUGER ELECTRON SPECTROSCOPY

For AES measurements, the powder samples were pressed into In foil. Samples prepared in this manner exhibited little charging, and were sufficiently densely packed so that no In could be detected. The measurements were made with a Physical Electronics single-pass cylindrical mirror analyzer (CMA) with a coaxial electron gun, in an ultrahigh vacuum chamber with a base pressure in the high 10^{-10} torr (10^{-8} Pa) range.

Electron beam voltage, current, and current density, chosen to minimize any beam effects, were 5 kV, 15 μA, and 0.05 A/cm^2, respectively; modulation was 3 eV. The surfaces were cleaned and depth profiles were obtained by Ar ion sputtering at a beam voltage of 2 kV, an ion current of 9 μA, and a current density of ~ 100 mA/cm^2, which corresponded to a calibrated sputtering rate of 40 Å/min for Ta_2O_5.

E. ELECTRON MICROSCOPY

A JEOL JEM 100-CX STEM was used for scanning electron microscopy (SEM) and transmission electron microscopy (TEM). A special method of coating SEM specimens with a thin layer of Pt allowed high resolution (30 Å) studies of the titanium oxide in the SEM mode at 50,000X magnification. SEM stereo pairs were obtained on a split CRT screen at a 12° tilt angle, allowing three-dimensional views of the oxide. For TEM, thin foils were prepared by ion milling. First, the original 1-mm thick pieces were mechanically thinned to about 5 μm, with the oxide side protected, and then 3-mm diameter discs were punched out of them. Milling was done on the Ti side, with a 5-kV Ar-ion beam hitting the sample at a 17° angle, for a few hours to a few days. Although the ion beam heated the specimen to nearly 100°C, it is believed that no artifacts were introduced. Stereo views were taken with the specimen tilted ± 6° around a tilt axis.

F. WATER IMMERSIONS

Each test specimen was placed in a glass tube filled with 20 ml of preheated distilled-deionized water (pH 7). The tubes were plugged with glass stopcocks and placed in heat blocks in a Fisher Isotemp Dry Bath. Exposure conditions were 60, 70, and 85°C ± 1°C for up to 1100, 500, and

230 hours, respectively. At given int vals, tubes were removed from the bath, and the specimens were washed ultrasonically in pure acetone and dried in a hot air flow. A second series of immersions was performed at 75, 85, and 95°C in a water bath with temperature control better than ± 0.5°C.

G. VACUUM HEATINGS

To isolate water-induced changes from pure heat effects, we performed a series of vacuum heatings on test coupons. Individual test specimens were vacuum heated in the chamber of a Physical Electronics Model 548 AES unit, at 10^{-5} Torr. Radiation was supplied by a heating element 0.5 cm away. The specimen was mounted on a rotating stainless steel carousel using two, small, stainless steel screws. Ceramic sleeves on the screws provided thermal insulation by acting as spacers between the specimen back and the carousel. A small thermocouple touching the specimen back monitored the temperature. Heating and cooling were rapid, at a rate of ~ 1°C/second. Exposure conditions were 100, 150, and 250°C for 1 hour and 100°C for 24 hours. The oxide mass/unit surface area ("equivalent thickness") was determined by AES depth profiling before and after each heat treatment.

III. AES LINE SHAPE STUDIES OF THE ANODIC AND TRANSFORMED OXIDE LAYERS

Theoretically, debonding between oxide and epoxy can occur without gross morphological changes in the oxide, of the sort described in our previous study[12]. The likelihood is that only the uppermost atomic layer of the oxide is actually bonded to the epoxy. Therefore, any change on an atomic scale in this layer will weaken the bond even if there is some temporary residual strength retention due to mechanical interlocking. Migration and crystallization, two examples of atomic-scale changes, are both temperature dependent and are influenced by the defect structure and disorder in the oxide film. Therefore, we suspect that at high temperatures, adhesive bonds will be seriously affected. However, we have observed changes in the oxides in the presence of water even at low (<100°C) temperatures, e.g., the formation of anatase crystallites and the disappearance of amorphous cells in a CAA film. Water apparently assists atomic-scale changes and even corrosion of Ti substrate under an anodic film at temperatures much lower than expected. The anodic film in particular and amorphous Ti oxides in general must have properties that make them susceptible to low temperature destabilization in water, since it is known that bulk, crystalline titanium oxides are very stable under similar conditions.

This analysis prompted us to investigate the nature of the CAA film and the corrosion product, using surface techniques that can best determine changes at various layers in the film.

Although X-ray photoelectron spectroscopy (XPS) is more commonly used to obtain chemical-state information on surface atoms, Auger electron

spectroscopy (AES) has also proven useful in a number of systems. AES is especially effective if one or both of the electrons involved in the transition originate(s) in the valence band. In such cases, the line shape can be used as a fingerprint of the particular chemical species or as a measure of the species-specific densities of states (DOS) of a compound. In particular, the Ti $L_{23}M_{23}V$ line shape has been applied as a fingerprint for Ti, TiO, Ti_2O_3, and TiO_2. The line shapes obtained by different laboratories on these oxides, however, do not always agree. Some discrepancies might have been caused by poorly characterized standards or surfaces, electron beam effects, or ion-induced reduction. Accordingly, we obtained our own line shapes from well-characterized materials and investigated possible electron and ion beam effects on the shapes. The line shapes were then used as a probe of the anodized samples.

A. RESULTS

The Ti $L_{23}M_{23}M_{23}$ and $L_{23}M_{23}V$ Auger line shapes for bulk TiO, Ti_2O_3, and TiO_2 in the rutile, anatase, and "amorphous" forms are shown in Fig. 1. Each surface represented in the figure was sputtered for 3 min. Although no significant differences can be seen among the different crystalline and "amorphous" phases of TiO_2 in the figure, the relative amplitudes of the features at ~ 411–415 eV and ~ 417–420 eV are an indication of the average stoichiometry of the sample. The peak amplitude at ~ 411–415 eV is lowest for the TiO_2 samples and approximately equal to that of the positive-going peak at 406–407 eV for TiO. These line shapes

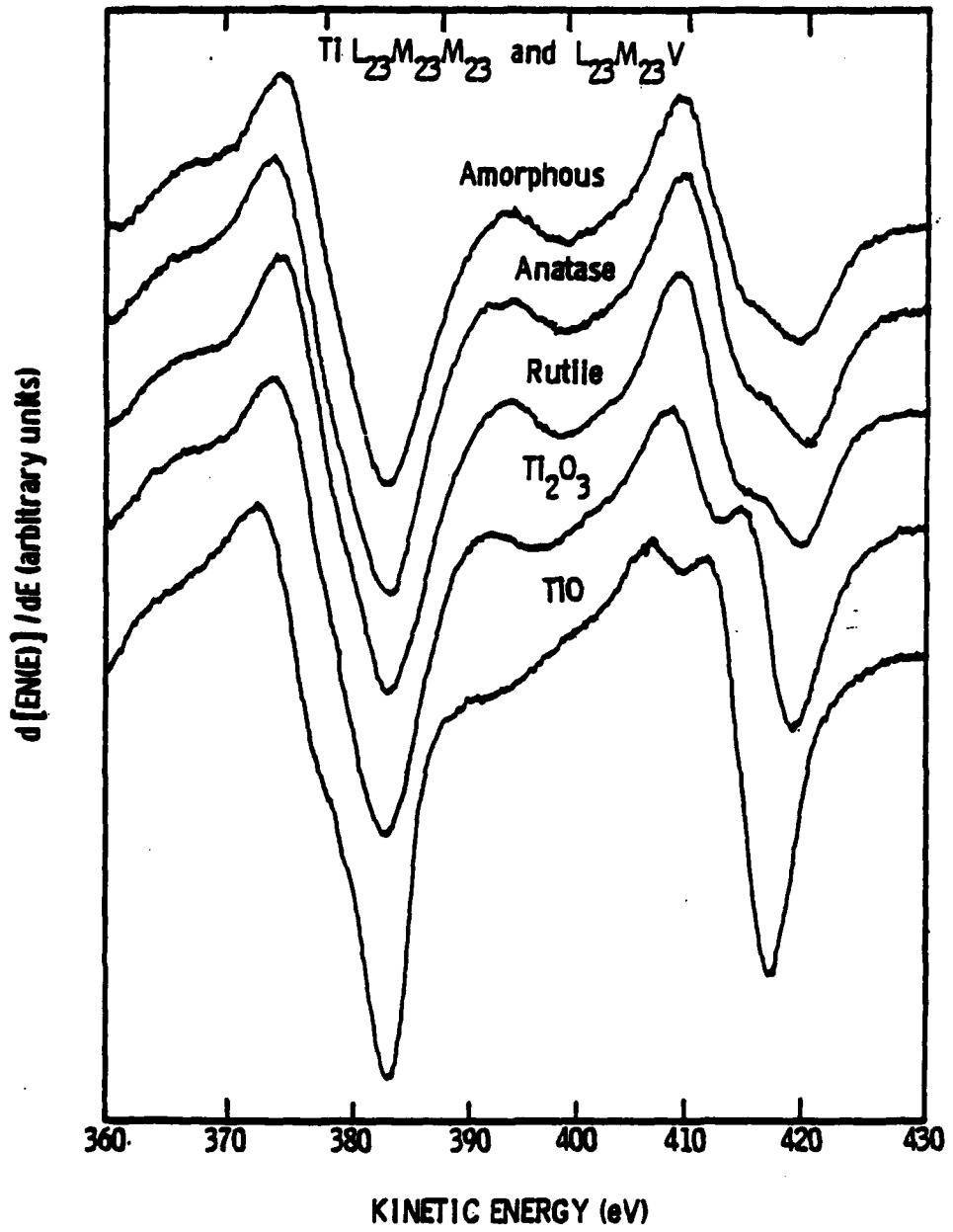

Figure 1. Ti $L_{23}M_{23}M_{23}$ and $L_{23}M_{23}V$ Auger line shapes for TiO, Ti_2O_3, and three phases of TiO_2: rutile, anatase, and "amorphous." The "amorphous" sample consisted, at least in part, of small (50 to 100 Å diameter) anatase crystallites. The measurements were made after 3 minutes of Ar ion sputtering. To correct for small differences in charging from sample to sample, each spectrum was shifted so that the Ti $L_{23}M_{23}M_{23}$ transition occurred at 383 eV.

are in general agreement with those reported by Grant et al.,[13] Gandon and Joud,[14] and Solomon and Baun,[15] but not with the assignments of Rao and Sarma.[16]

Although one can determine the average stoichiometry of the surface from these line shapes, the specific phases present are not distinguishable. For example, the spectra from a 1:1 molar mixture of TiO and TiO_2 (anatase) and Ti_2O_3 can be compared in Fig. 2. In both spectra, the shoulder at 411-415 eV approaches the background level and the line shapes are quite similar.

Several investigators have reported electron and/or ion beam reduction of TiO_2 to Ti_2O_3 or TiO, or of Ti_2O_3 to TiO.[15-19] Roche et al.[5] and Armstrong and Quinn,[20] on the other hand, have indicated that beam effects are not observed under some conditions. The amount of any such damage would be a function of beam voltage, current density, and measurement time, and would vary from laboratory to laboratory. To determine the extent of beam effects for our measurements, we examined our standards after different exposures to the electron and ion beams. Selected line shapes and O KVV/Ti $L_{23}M_{23}M_{23}$ peak-to-peak height ratios from these tests are shown in Figs. 3, 4, and 5. These line shapes and similar ones from the other standards — Ti_2O_3, rutile, and "amorphous"

---

13 J.T. Grant, T.W. Haas, and J.E. Houston, J. Vac. Sci. Technol. 11, 227 (1974).
14 J. Gandon and J.C. Joud, J. Less-Com. Met. 69, 277 (1980).
15 J.S. Solomon and W.L. Baun, Surf. Sci. 51, 228 (1975).
16 C.N.R. Rao and D.D. Sarma, Phys. Rev. B 25, 2927 (1982).
17 S. Thomas, Surf. Sci 55, 756 (1976).
18 M.L. Knotek and J.E. Houston, Phys. Rev. B. 15, 4580 (1977).
19 H.J. Mathieu, J.B. Mathieu, D.E. McClure, and D. Landolt, J. Vac. Sci. Technol. 14, 1023 (1977).
20 M.R. Armstrong and R.K. Quinn, Surf. Sci. 67, 451 (1977).

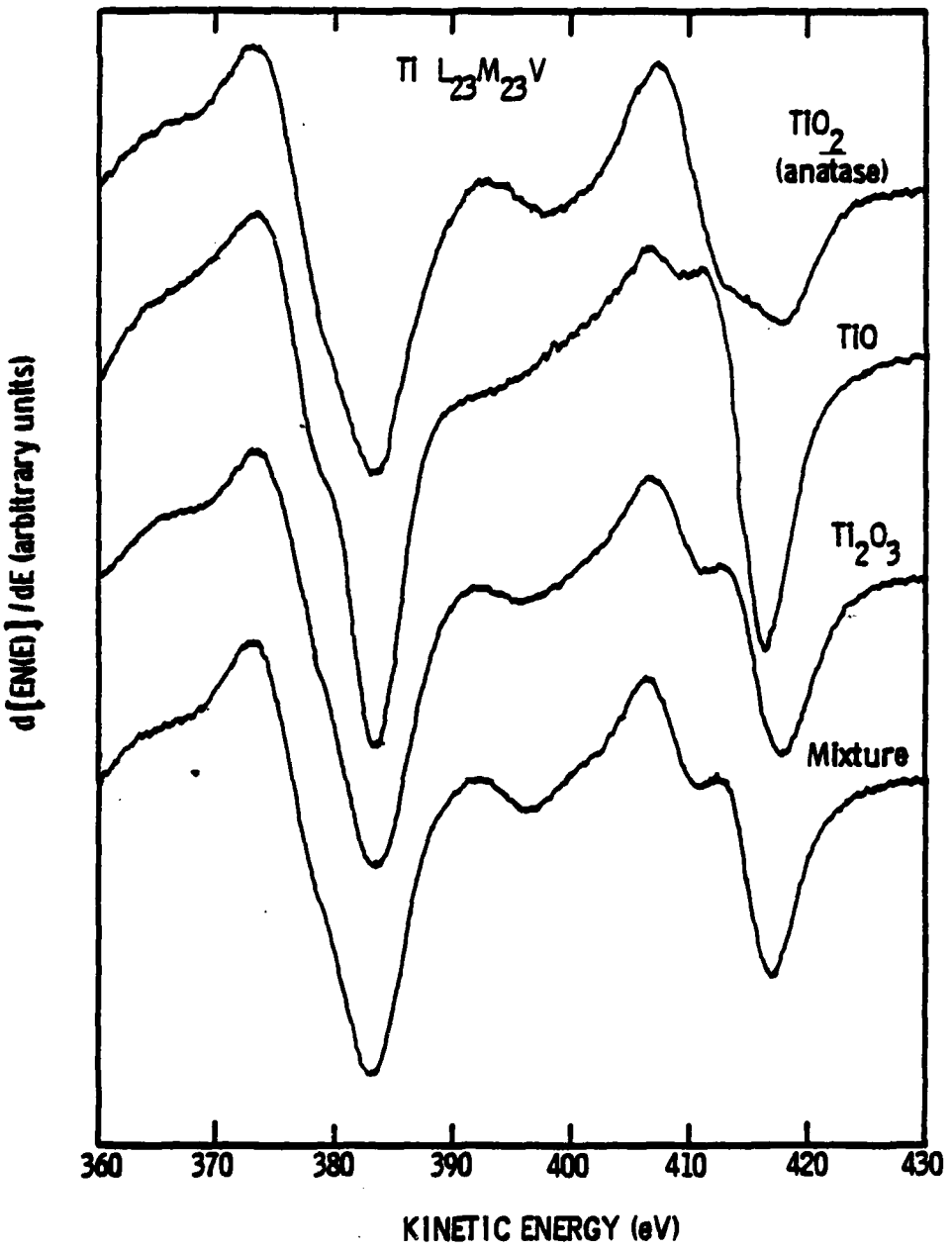

Figure 2. Ti $L_{23}M_{23}M_{23}$ and $L_{23}M_{23}V$ Auger line shapes for anatase, TiO, Ti_2O_3, and a 1:1 molar mixture of anatase and TiO. The measurements were made after 3 seconds of Ar ion sputtering.

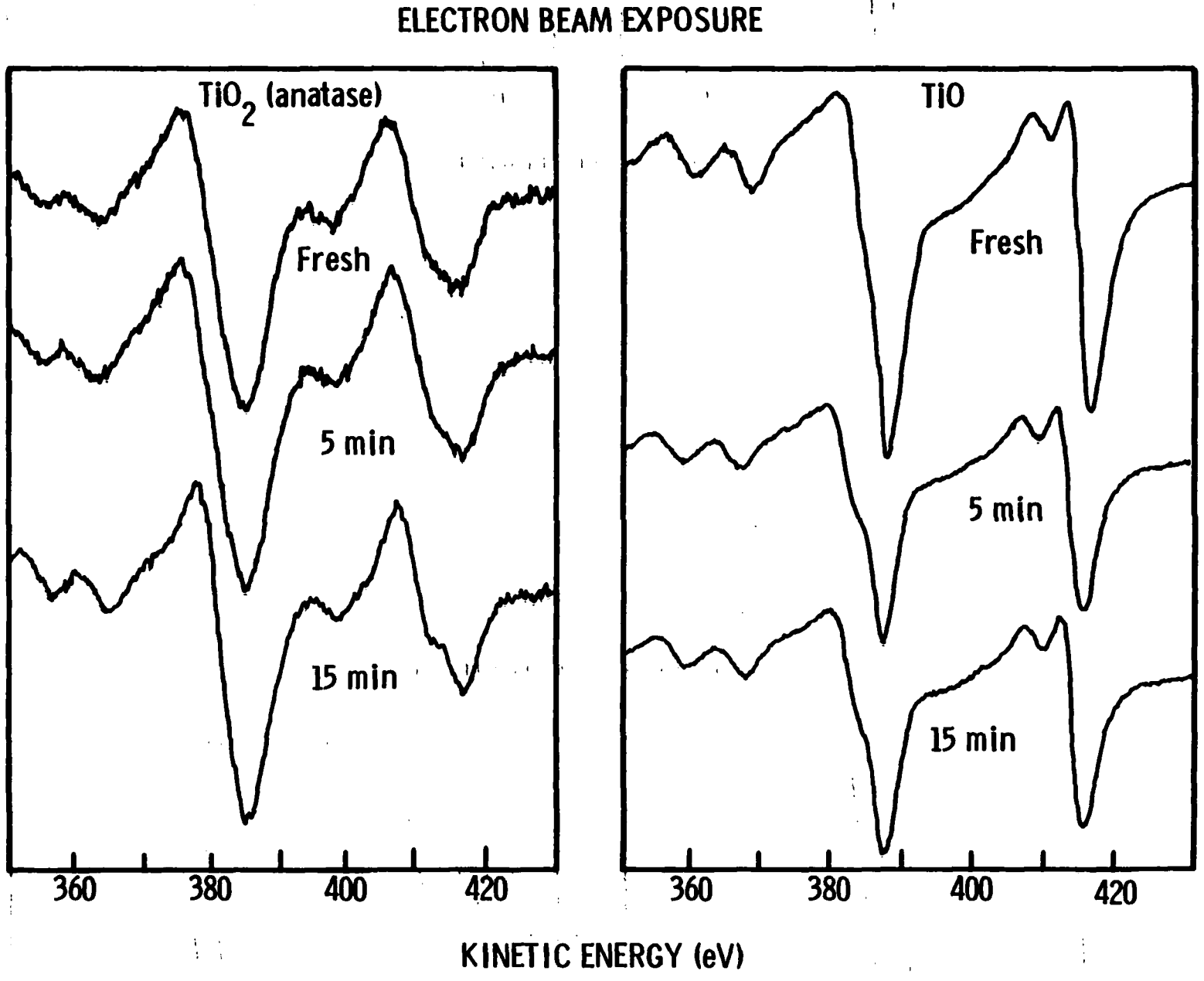

Figure 3. Ti $L_{23}M_{23}M_{23}$ and $L_{23}M_{23}V$ Auger line shapes for anatase and TiO for different exposures beam (5 keV, 15 μA, ~ 0.05 A/cm^2).

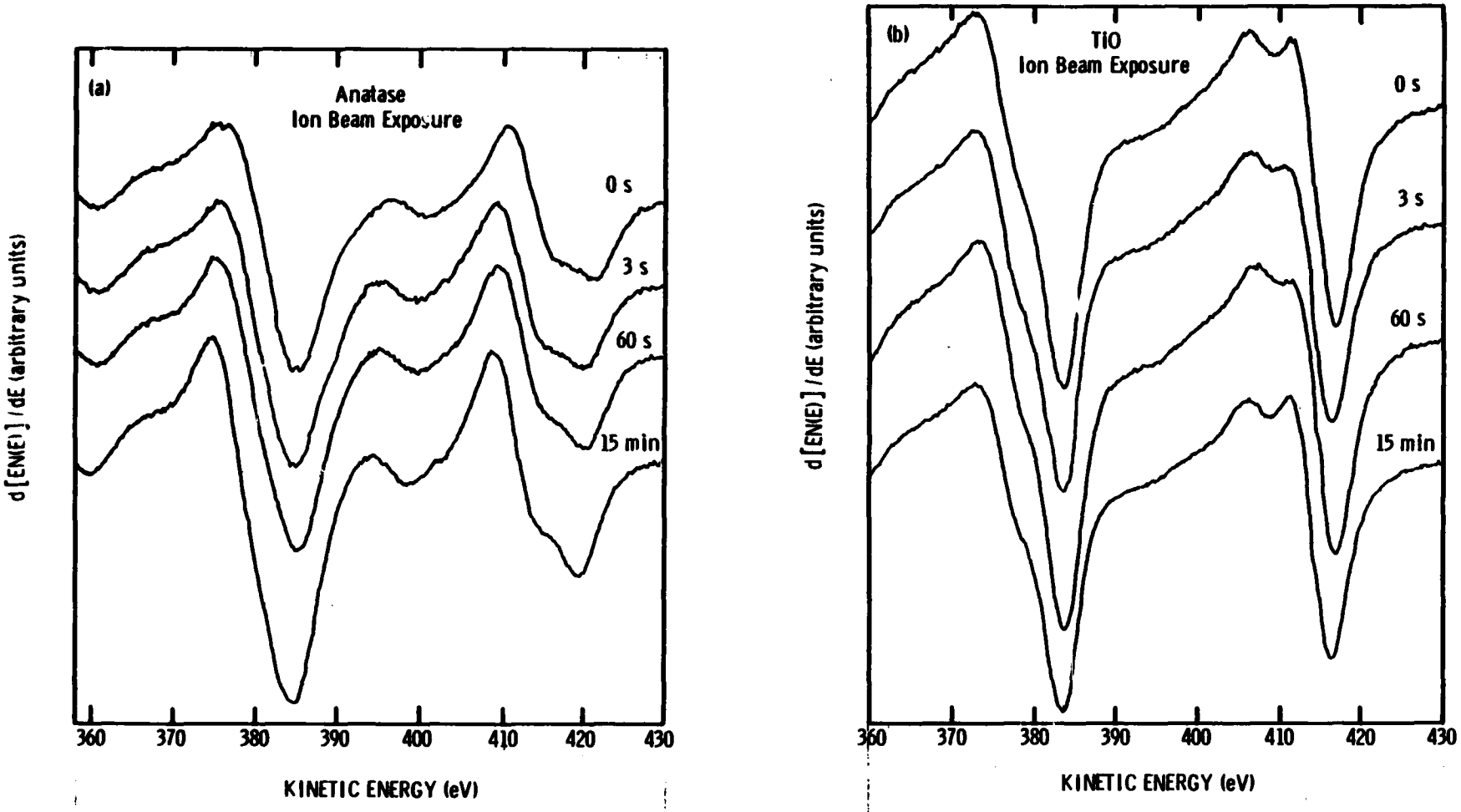

Figure 4. Ti $L_{23}M_{23}M_{23}$ and $L_{23}M_{23}V$ Auger line shapes for (a) anatase and (b) TiO at different exposures to the Ar ion beam (2 keV, 9 μA, ~ 100 mA/cm^2).

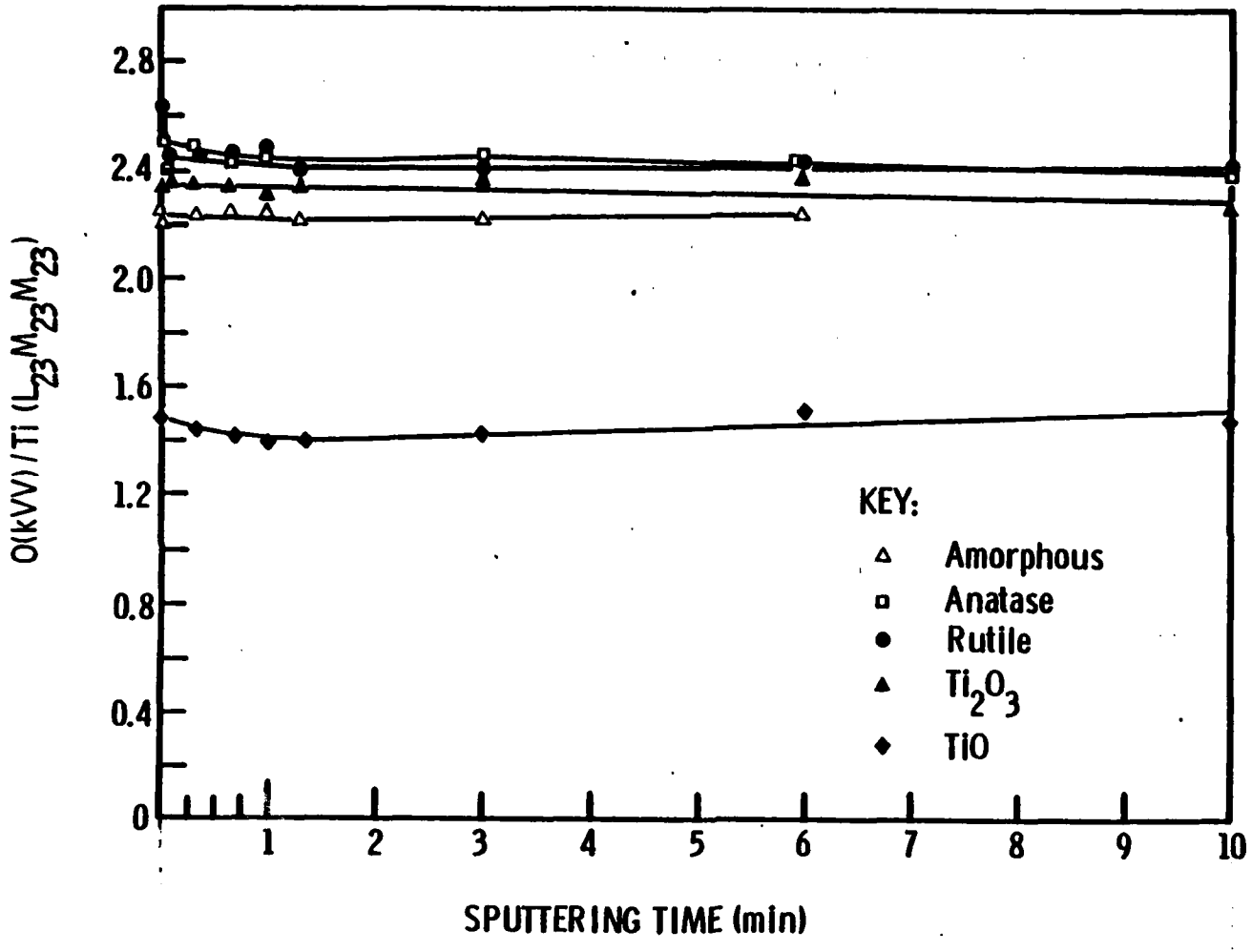

Figure 5. Ratio of O KVV and Ti $L_{23}M_{23}M_{23}$ peak-to-peak heights for TiO, Ti_2O_3, rutile, anatase, and "amorphous" TiO_2 as a function of sputtering time.

TiO_2 — do not change appreciably with up to a 15-minute exposure to the electron beam or a 20-minute exposure to the ion beam. Similarly, the O/Ti peak-to-peak ratios change very little, except for an initial decrease for anatase which is attributed to an adsorbed layer of H_2O or other oxygen-containing contamination. These results appear to indicate that our experimental conditions were sufficiently gentle to prevent reduction of the oxides; that this might not have been true for amorphous samples, however, will be shown below.

Although the stoichiometry can be determined from the Ti $L_{23}M_{23}V$ line shape, it is difficult to do so from the $L_{23}M_{23}M_{23}$ peak-to-peak height ratio, since this parameter does not scale linearly with the O/Ti ratio (Fig. 5). Indeed, it may not be possible to distinguish between Ti_2O_3 and TiO_2 using this ratio. This behavior contrasts with that observed by Gandon and Joud,[14] who reported a linear relationship between the initial peak-to-peak height ratio and the stoichiometric ratio. However, it agrees with the results of Grant et al.,[13] who reported that the deviation from linearity was due to the sensitivity of the derivative spectrum to line shape changes. Proportionality, however, should be achieved by taking the second integral of the derivative spectrum [the N(E) peak area], preferably after appropriate data analysis to remove effects of electron inelastic scattering.

The thin films exhibited a different behavior upon ion sputtering than the standards. The films produced by chromic acid anodization (CAA), anodization followed by hot water immersion, and RSD, exhibited spectra which initially were generally consistent with stoichiometric TiO_2. Although the unsputtered surfaces of the two anodized samples

exhibit high O/Ti peak-to-peak height ratios (Fig. 6), which we attribute to adsorbed H_2O, the line shapes (Fig. 7a and b) indicate an oxygen-deficient TiO_2 stoichiometry. With sputtering, the O/Ti peak-to-peak height ratio quickly decreases to a value between those of TiO and Ti_2O_3, as do the line shapes. Similar results were also observed for other CAA samples undergoing different heat treatments.

The RSD oxide film initially exhibits a TiO_2-like line shape and an O/Ti peak-to-peak height ratio like that of the TiO_2 standards (Figs. 6 and 7c). After sputtering, however, this peak-to-peak height ratio decreases to a value between those of TiO and Ti_2O_3. The line shapes also change until they, too, are intermediate between those of TiO and Ti_2O_3.

In an attempt to substantiate these apparent stoichiometric changes, we performed TEM and electron diffraction on the thin films. We found that the water-immersed CAA surface (see Section IV) consisted of a corrosion product layer of anatase crystallites (~ 2000 Å long and a few hundred angstroms wide) with a cubic TiO phase at their base -- a structure that is consistent with the Auger results. Without having done a quantitative analysis to determine the relative proportions of TiO and TiO_2, however, these measurements are not sufficient to verify that the Auger results accurately represent the sample stoichiometry rather than the effect of ion beam-induced reduction, although they very likely do.

The original CAA oxide and the RSD oxide, on the other hand, were found to be amorphous, except for a trace of TiO crystallites in the CAA oxide (Fig. 8, a and c), so electron diffraction could not be used to identify the phases present. [The presence of TiO crystallites on

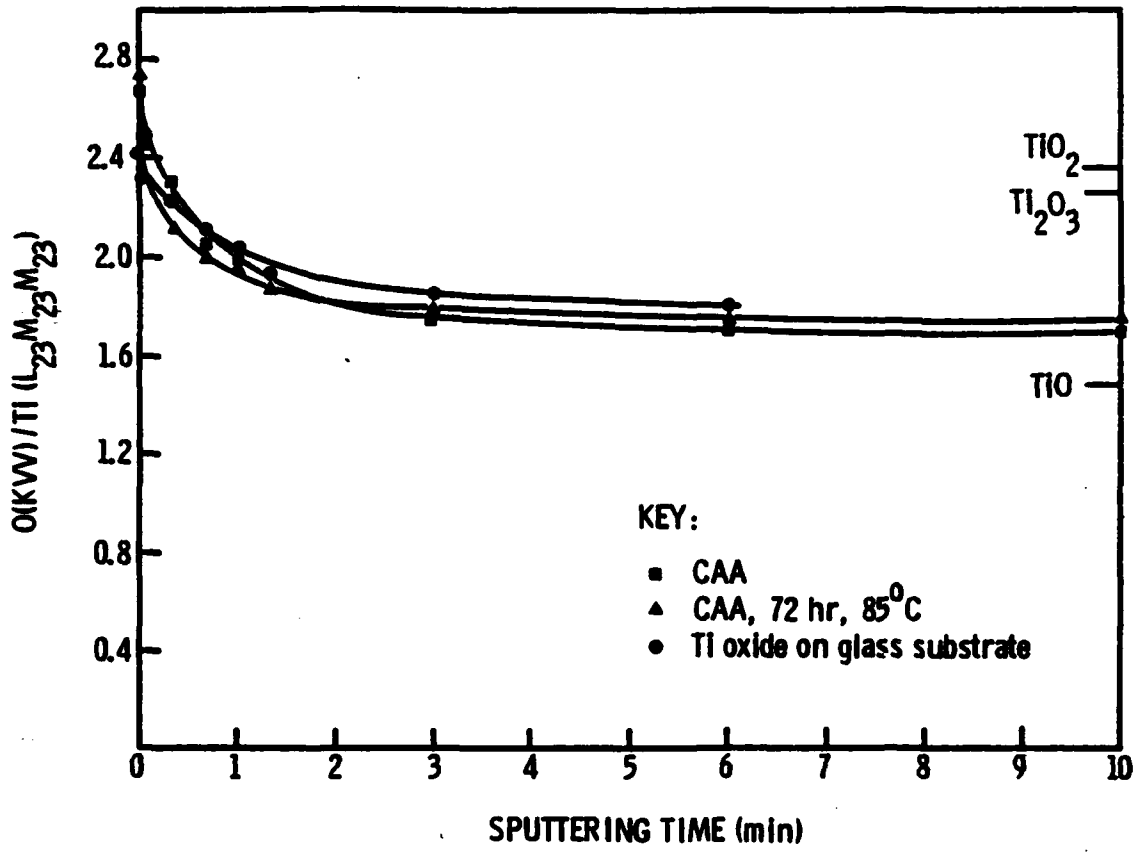

Figure 6. Ratio of O KVV and Ti $L_{23}M_{23}M_{23}$ peak-to-peak heights for chromic-acid-anodized (CAA) oxide before and after immersion in 85°C water for 72 hr, and for a reactive sputter-deposited (RSD) oxide on a glass substrate.

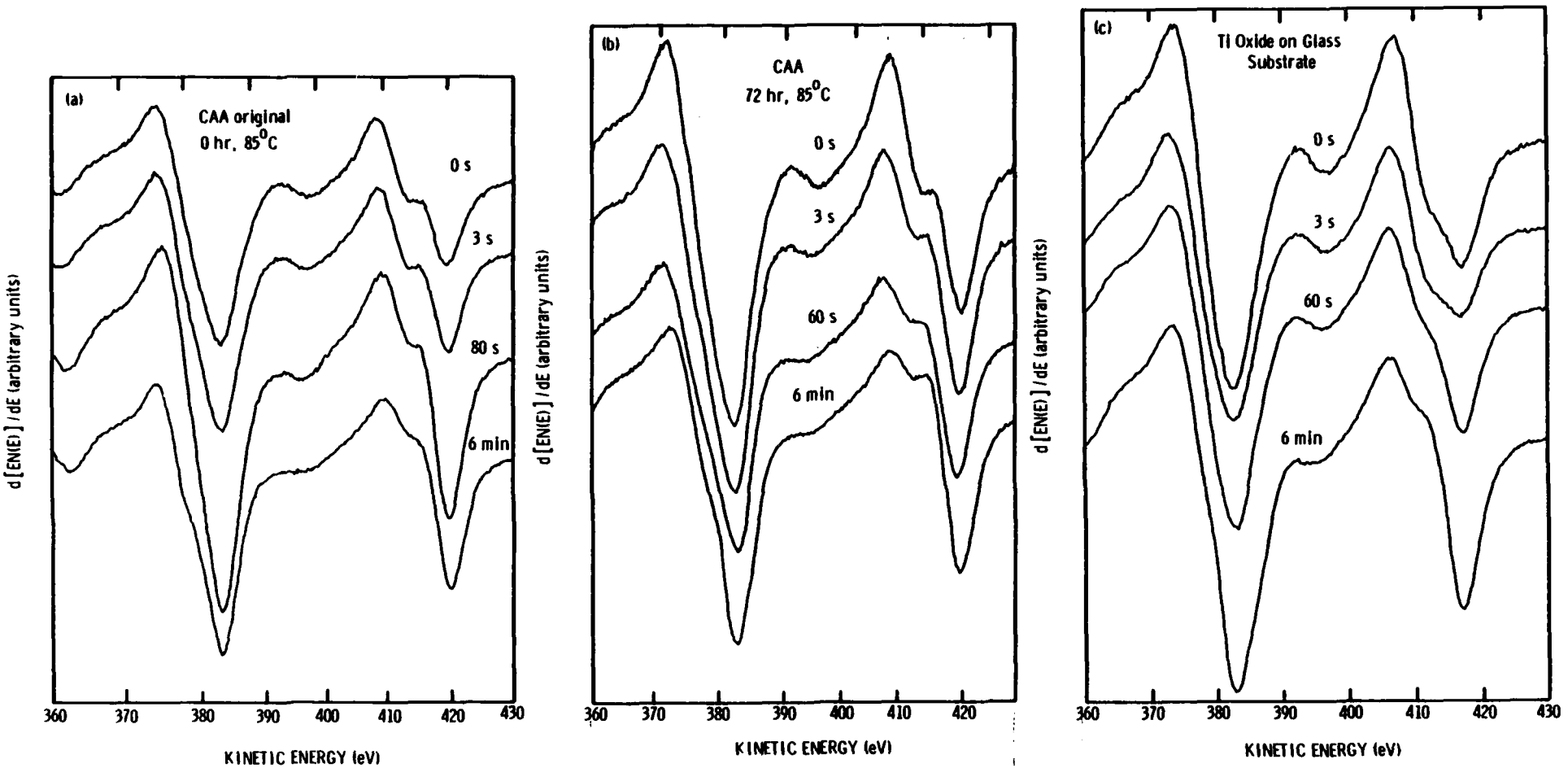

Figure 7. Ti $L_{23}M_{23}M_{23}$ and $L_{23}M_{23}V$ Auger line shapes for CAA (a) before and (b) after immersion in 85°C water for 72 hr, and (c) for a RSD oxide on a glass substrate as a function of sputter time. The line shapes indicate an apparent ion beam-induced reduction.

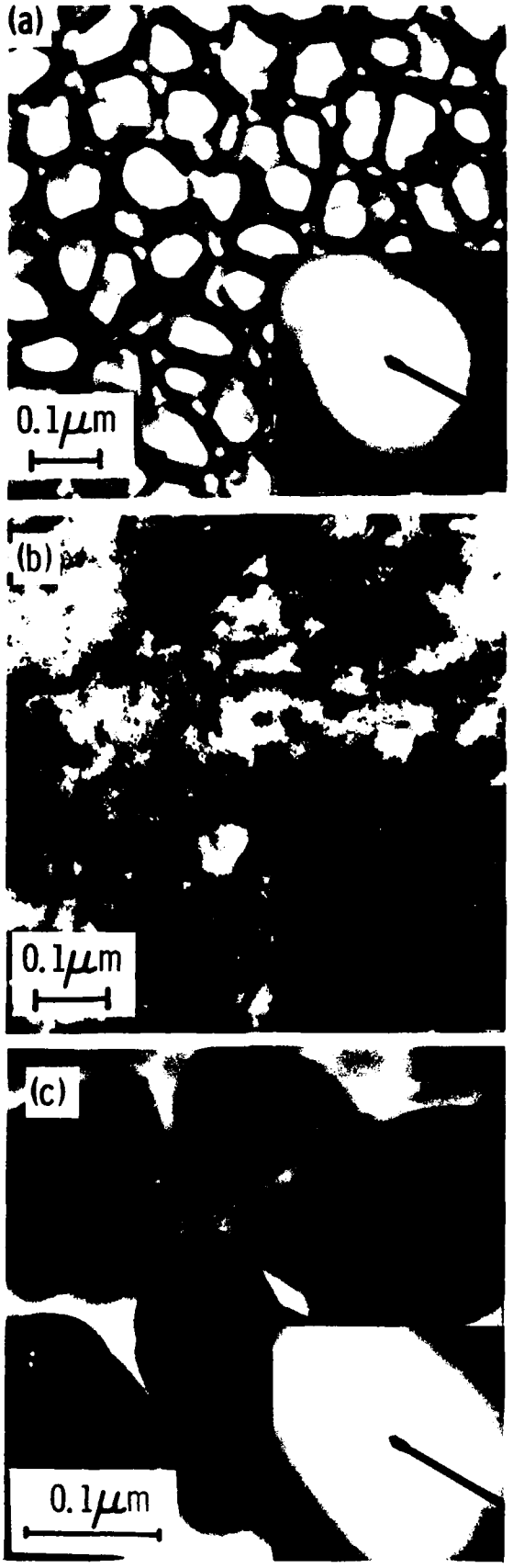

Figure 8. Transmission electron micrographs and electron diffraction patterns for CAA oxide (a) before and (b) after immersion, and (c) for the RSD oxide.

the water-immersed CAA sample could not be used to infer the presence of amorphous TiO on the original CAA oxide. The TiO crystallites may have been produced by water penetrating the porous oxide and reacting with the metal substrate.]

Since the apparent reduction of the two amorphous oxide films could reflect either the actual stoichiometry, a sputtering artifact (reduction), or a combination of the two, we attempted to distinguish between these possibilities. Another RSD oxide was deposited onto an aluminum substrate and exposed to the atmosphere for 20 minutes. An additional 770 Å of oxide was then deposited, and the sample was analyzed by AES.

If the results on the initial, single-layer RSD oxide represented the true stoichiometry, i.e., Ti_2O_3 with a TiO_2 overlayer formed by exposure to the atmosphere, a layer of TiO_2 would be seen between the two layers of Ti_2O_3 in the two-stage film. On the other hand, if the original results were due to experimental artifacts, no TiO_2 would be seen on the two-stage sample except at the surface. To ensure detection of any TiO_2 interlayers present, line shapes and peak-to-peak height ratios were measured every 20 Å in a 300 Å region centered on the expected depth of the interlayer; selected line shapes from this series are shown in Fig. 9. No indication of a buried TiO_2 layer was found in any of the line shapes or peak-to-peak height ratios. (The shoulder at ~ 411-415 eV, approximately midway between the positive- and negative-going peaks, indicates that Ti_2O_3 is less distinct in these spectra than in others presented due to incorporation into the oxide of carbon from the mounting adhesive during the deposition procedure. However, because the line shape

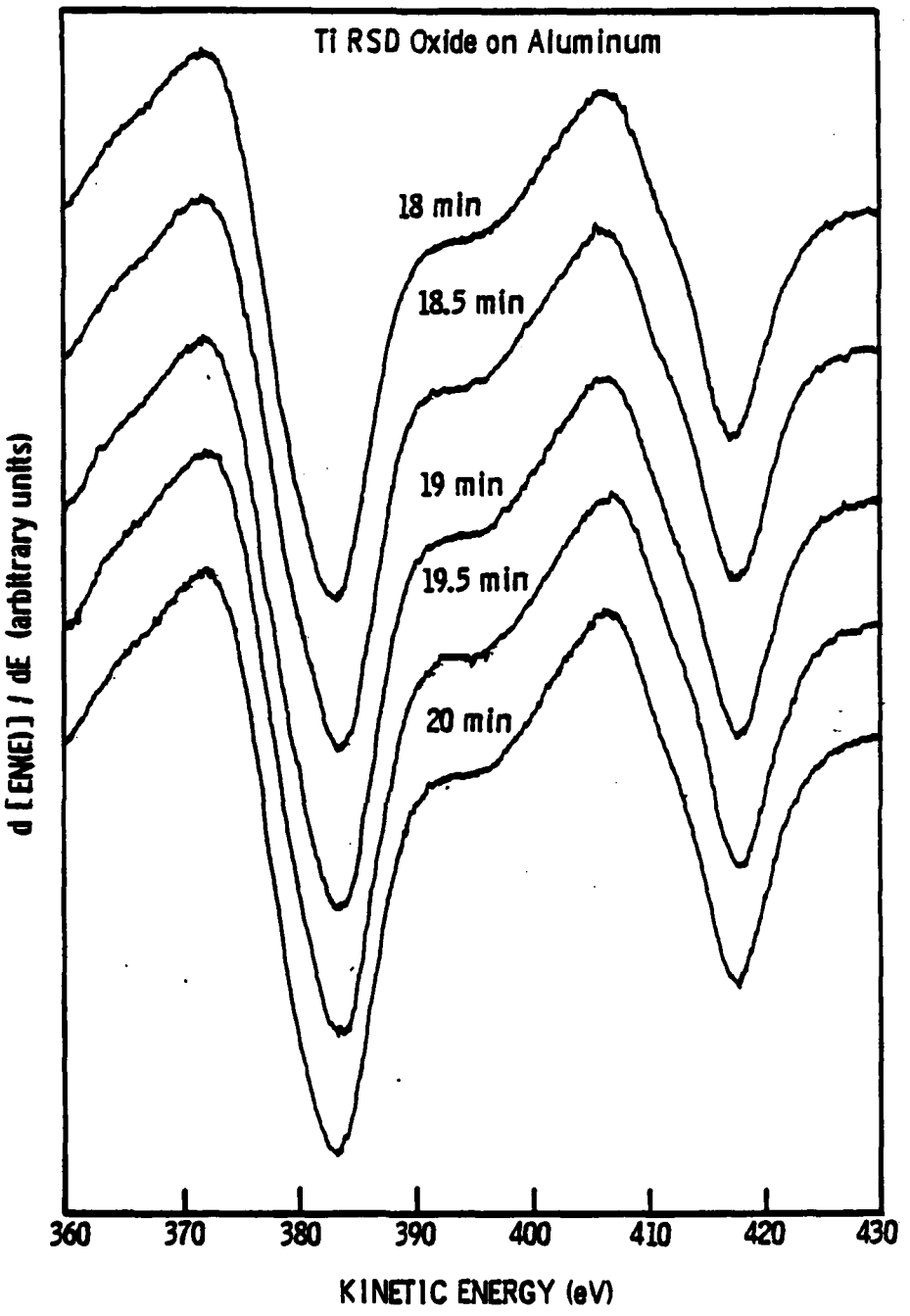

Figure 9. Selected Ti $L_{23}M_{23}M_{23}$ and $L_{23}M_{23}V$ Auger line shapes for the two-stage RSD oxide (see text). Sputtering time during analysis is indicated by each curve. The shoulder at ~ 411–415 eV occurs near the background level, indicating Ti_2O_3 stoichiometry.

exhibited the same initial behavior as those of the other RSD oxides, the carbon is believed not to have affected the position of the shoulder nor the conclusions derived from the data.)

These results suggest strongly that a sputter-induced reduction is responsible for most of the phenomena observed on the amorphous oxides. However, as discussed in Section V, they still leave open the possibility that amorphous TiO_2 is nonstoichiometric, due to lattice defects (oxygen vacancies). In any event, the amorphous titanium oxides exhibited stoichiometry changes upon ion bombardment, whereas the crystalline oxides did not. Whether this points to weaker Ti-O bonds in amorphous films or to inherently more defects, it reinforces the likelihood that more changes due to heating will occur in amorphous than in crystalline oxides. It also suggests that micro-corrosion in water will be aided by a highly defective amorphous layer in contrast to a more perfect, stoichiometric crystalline oxide. For adhesive bonding, a crystalline titanium oxide layer is therefore preferable to an amorphous film.

IV. TRANSFORMATIONS IN AN ANODIC OXIDE

In addition to providing chemical-state and some structural information, AES can be used for quantitative measurements of oxide mass/unit area of surface in corrosion studies. The method is based on measuring the time needed to ion-sputter away the oxide layer at a known rate to reach the oxide-substrate interface. A typical AES depth profile is shown in Fig. 10. In general, all profiles exhibit three regions: an oxide region, I; an oxide/metal transition region, II; and a metal region, III. An equivalent oxide thickness is estimated by multiplying the sputtering time taken to reach the middle of region II by a calibrated sputtering rate. Since the calibration is performed on a fully dense oxide with a thin oxide/metal transition region, the equivalent thickness underestimates the real thickness by a factor of 2 to 4 depending on the oxide porosity. However, because the method gives a very good indication of the oxide mass/unit area of the surface and can be used to monitor mass changes, it was therefore used to follow the oxide transformations and substrate corrosion in water immersions, as discussed in the following chapter.

A. WATER IMMERSIONS

In our previous report,[12] we described the morphological changes observed on four different pretreated surfaces after hot water immersion. In general, we found the surfaces covered with anatase crystallites. It was unclear if the new phase was formed by corrosion of the base metal, transformation of the original oxide, or both. In this study we attempted to further clarify these water-induced changes.

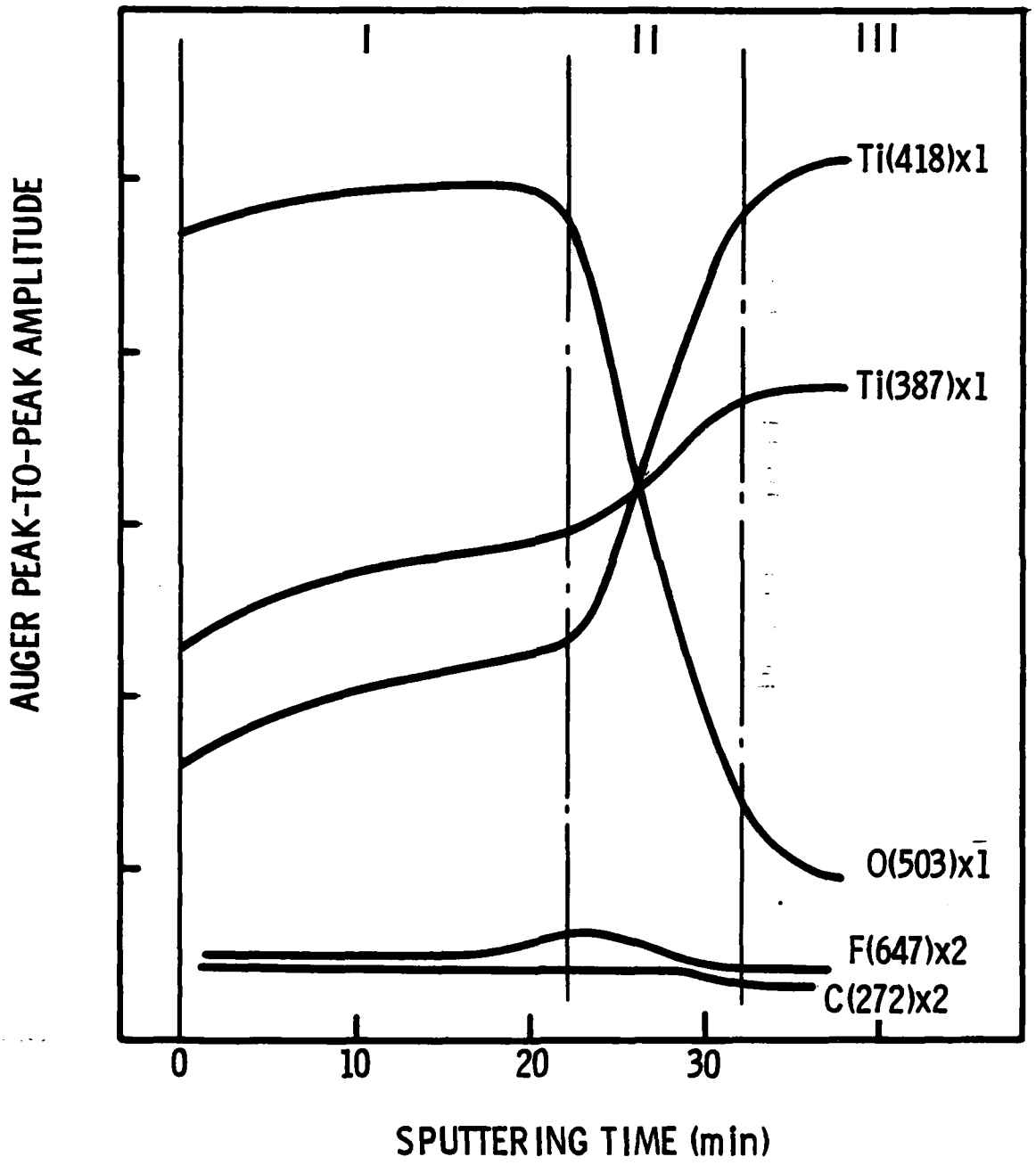

Figure 10. AES depth profile of the as-prepared CAA oxide.

Two series of immersions were performed, one at 60, 70, and 85°C, and the other at 75, 85, and 95°C. In all cases, AES depth profiling was used to measure the oxide mass/unit area of surface. In the first series, Fig. 11, the mass generally remained unchanged after 60 and 70°C immersions. At 85°C, however, (Fig. 12) after a period of little change, the mass increased drastically, the increase coinciding with the formation of an anatase layer. In the second series, mass increases were observed at each temperature (75, 85, and 95°C) and the rate of increase was strongly dependent on temperature.

Electron microscopy results for many of the immersed specimens reinforced the view that both substrate corrosion and an oxide transformation occur by a highly temperature-sensitive process. A number of TEM bright-field micrographs of the anodic layer under various immersion conditions are shown in Fig. 13. At the lower (60 and 70°C) temperatures, even the longest immersions failed to cause a noticeable change in the original morphology, although some formation of small TiO crystallites was indicated by SAD patterns (e.g., Fig 13 b,d). At 85°C there were marked morphological and structural changes (Fig. 13 f). After immersions that resulted in an increased oxide mass, the original anodic layer disappeared by being either consumed or filled in with the anatase crystallites. Since the cell structure is no longer visible in Fig. 13 f, the assumption that the amorphous oxide was consumed in a transformation to anatase is quite reasonable. However, the net mass increase could also occur by additional oxide formation through corrosion of the substrate.

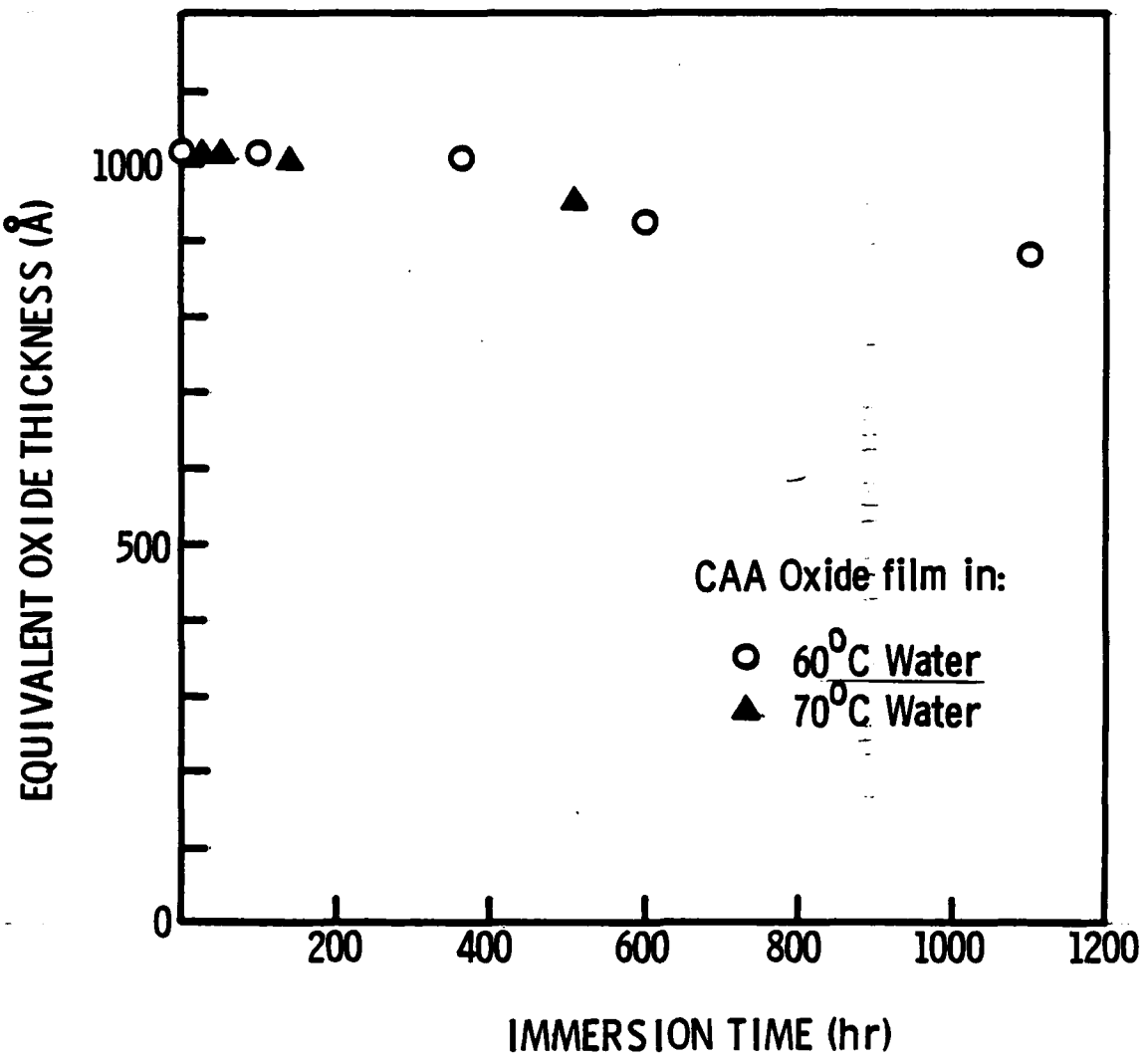

Figure 11. Equivalent oxide thicknesses (mass/unit area) of CAA oxides immersed in water at 60 and 70°C.

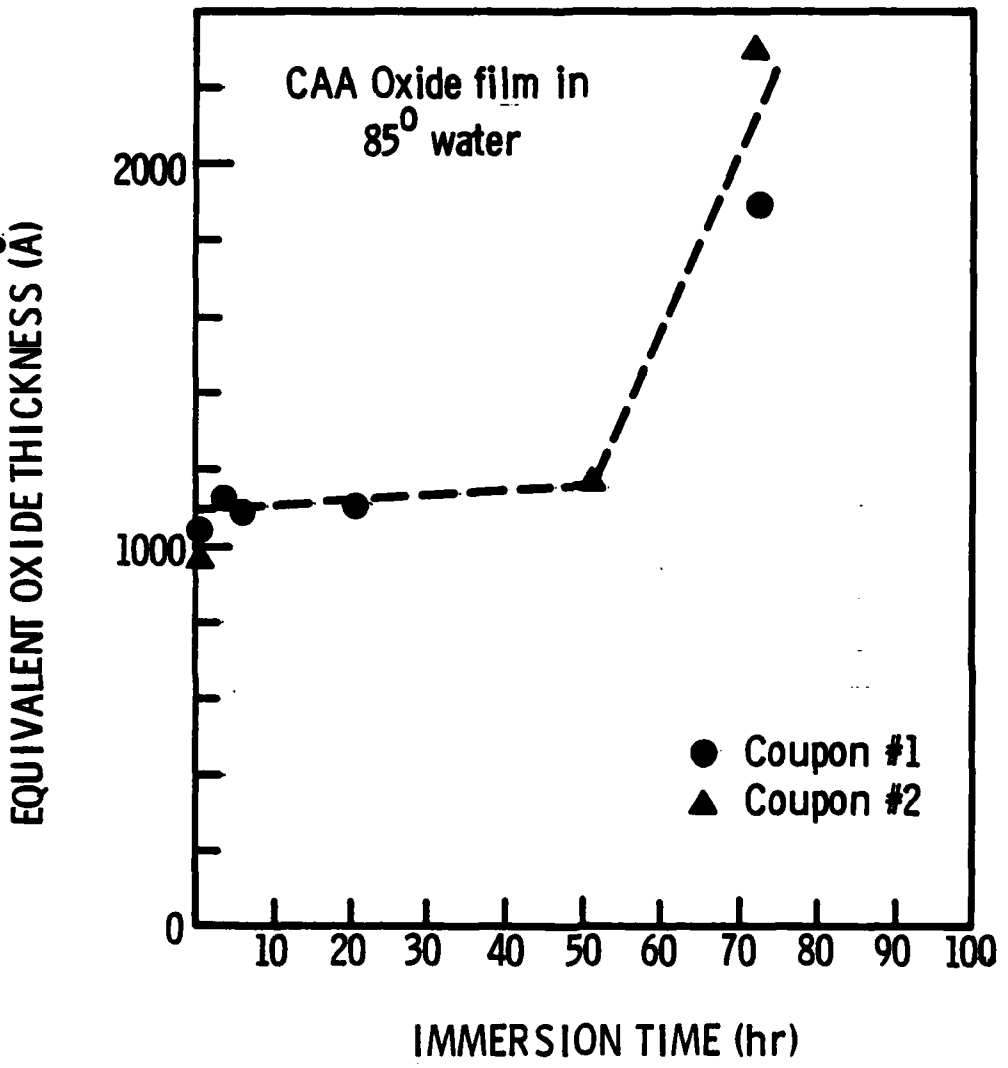

Figure 12. Equivalent oxide thicknesses (mass/unit area) of CAA oxides immersed in water at 85°C.

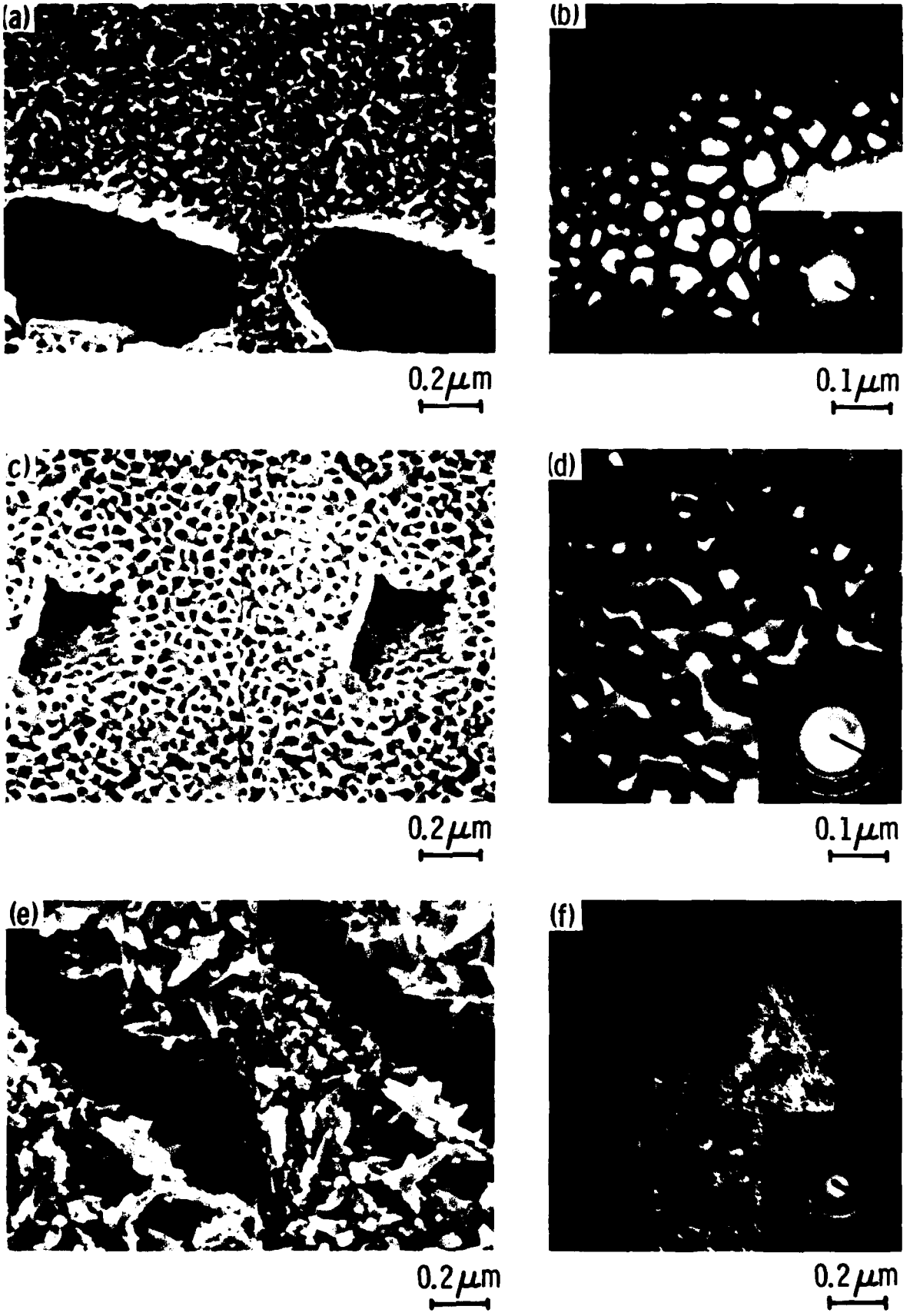

Figure 13. SEM stereo pairs and TEM/SAD views of immersed oxides after 1100 hours at 60°C (a,b), 500 hours at 70°C (c,d), and 72 hours at 85°C (e,f).

This latest conclusion is supported by data from "clean" Ti surfaces immersed in water. Figure 14 shows the surface of a specimen that was degreased and pickled to remove the natural oxide, and then immediately immersed in water for 24 hours at 95°C. The same growth of anatase crystallites that was seen on anodized surfaces is evident here. Since no oxide was present prior to immersion, the formation and growth of anatase implies a corrosion process. A similar case was reported by Fraker and Ruff[21] for Ti immersed above 150°C in various pH solutions. However, as far as we are aware, this is the first case of Ti corrosion in pure water detected below 100°C.

Adhesion of the crystallites to the substrate was checked by a simple tape test. The tape was pressed against the coupon surface and then peeled off. Subsequent high resolution SEM showed no significant morphological changes, indicating that the crystallites were not merely precipitates lying on the surface but a phase nucleating on and growing from the substrate.

B. VACUUM HEATING

According to our findings, the combined oxide crystallization/corrosion process in water is strongly temperature dependent, which raises the possibility that some changes are caused by a purely thermal effect. To isolate it, we vacuum heated some anodized coupons and monitored the morphology, crystal structure, and chemical composition. The conditions chosen were 100, 150, and 250°C for 1 hour and 100°C for 24 hours. After heating, the oxides were depth profiled with AES. As seen

---

21 A.C. Fraker and A.W. Ruff, Corrosion Sci, 11, 763 (1971).

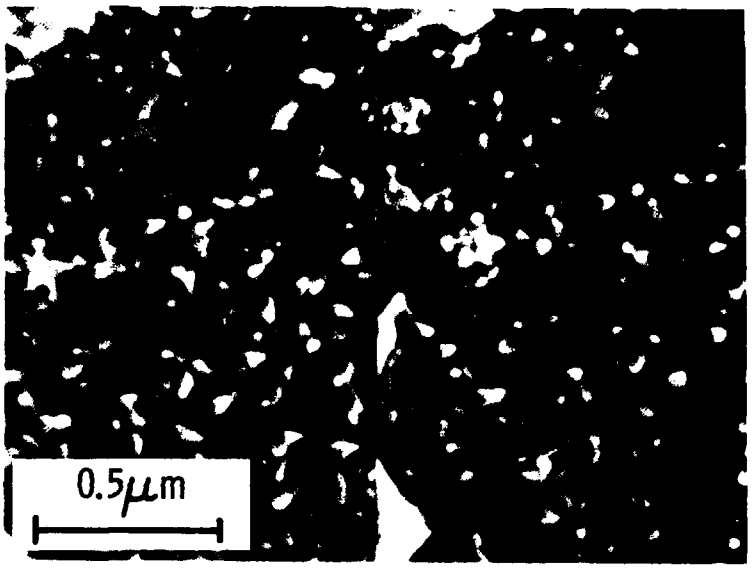

Figure 14. "Clean" Ti-6-4 surface after immersion in water at 95°C for 24 hours. Note the resemblance between this morphology and that of Fig. 13e.

in Fig. 15, the oxide mass after the 1-hour runs remained unchanged at all temperatures, and, if anything, seemed to decrease slightly after the 24-hour run. No chemical changes that could arise from diffusion of substrate elements into the oxide were detected, except for a possible slight increase in Al concentration in the long (24-hour) exposure at 100°C. Scanning electron microscopy stereo views taken after each run showed that oxide morphology remained unchanged; typical cells and fingers were seen on all surfaces. Clearly, the crystallite growth and mass increase on the immersed surfaces required the presence of water and did not occur solely through a solid-state transformation.

The formation of new oxide in hot water, which can be considered corrosion on a microscopic scale, is evidence of the permeability of the anodic film to various diffusing species, and also of its instability. The aspect relevant to adhesive bonding is again the stability of the uppermost atom layer in the oxide. In view of the results presented here, this layer can be expected to debond after long exposures in water, possibly because of the migration of O atoms away from the epoxy-oxide interface or of vacancies in the film toward the interface. Such atomic movements can be expected long before the detection of anatase crystallites. The exact role of the water is not clear; it possibly is a source of O atoms or a catalyst in the weakening of O-Ti bonds. Even without water, thin anodic films can be expected to crystallize if the temperature is raised above a certain point,[22] although it is unclear what morphological changes will occur following crystallization.

---

22 M. Shiojiri, J. Phys. Soc. Japan, 21, 335 (1966).

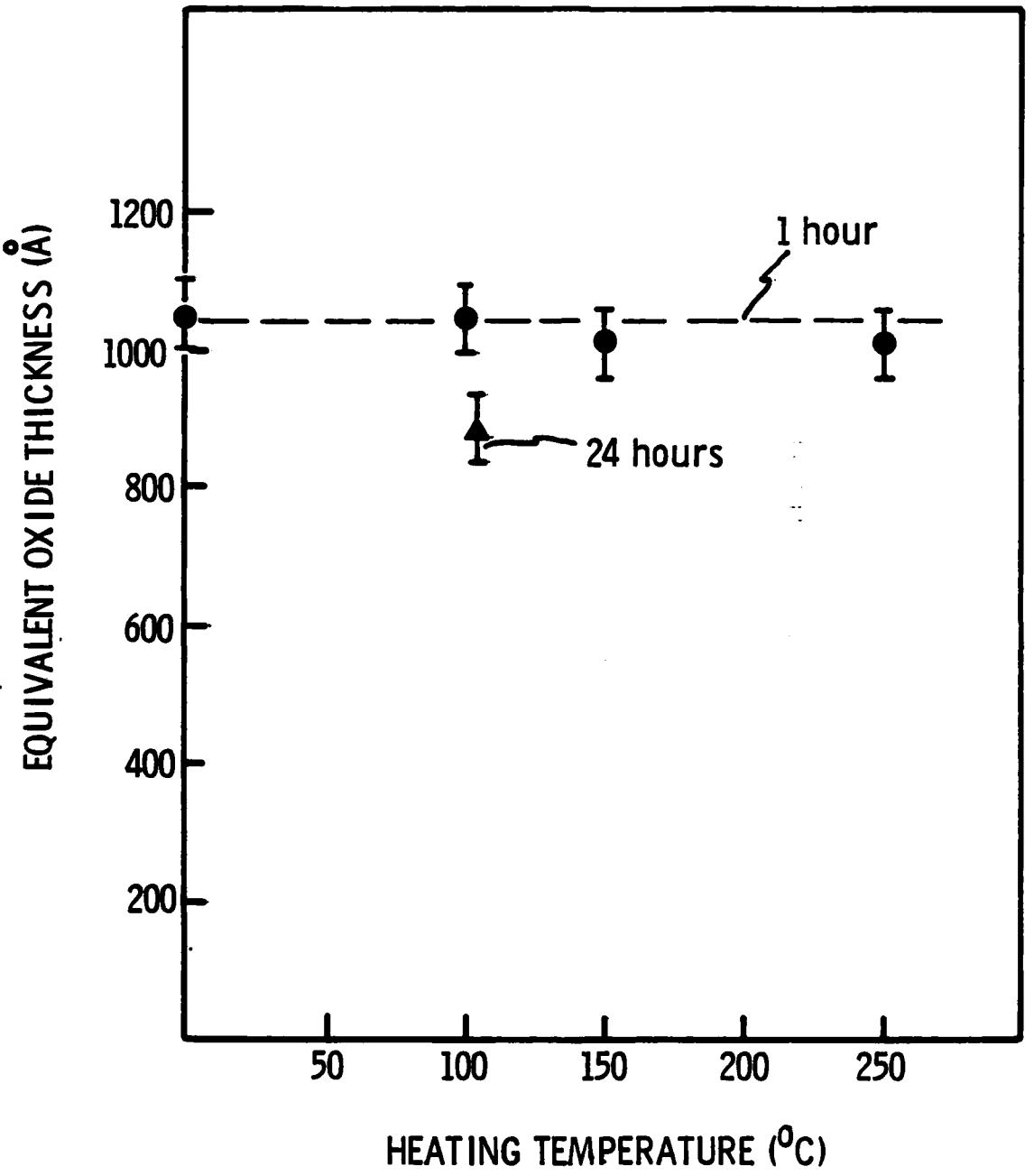

Figure 15. Equivalent oxide thicknesses (mass/unit area) of CAA oxides heated in vacuum.

V. DISCUSSION

The AES line shape studies indicate that during depth profiling a sputtered-induced reduction occurs in amorphous thin films that does not occur in crystalline powders. This reduction was observed in RSD films deposited on glass and aluminum as well as titanium. Because it occurred within the first 50 Å regardless of oxide thickness, it therefore is unrelated to the substrate. Most probably it results from the amorphous nature of the thin films and points to weaker bonds between Ti and O atoms which allow easier preferential sputtering of O atoms, in accordance with the predictions of Kelly's proposed model [23]. Such preferential sputtering would not be expected in the crystalline polymorphs, particularly rutile, which have a higher heat of formation.[24]

Altogether, these results seem to confirm the opinion that amorphous films are inherently less stable thermodynamically than their crystalline forms.[25] It is tempting to project the decreased stability of amorphous oxides to a humid environment, and conclude that, at least for titanium, it will lead to degradation of adhesive bonds. We have identified four possible mechanisms leading to degradation: dissolution, surface migration and solid-state crystallization of the oxide, and diffusion of various species through the oxide leading to micro-corrosion of the base metal.

---

23 R. Kelly, Surf. Sci. 100, 85 (1980).
24 F.D. Rossini, D.D. Wagman, W.H. Evans, S. Levine, and I. Jaffe, Selected Values of Chemical Thermodynamics Properties (National Bureau of Standards, Washington, DC, 1952).

V. DISCUSSION

The AES line shape studies indicate that during depth profiling a sputtered-induced reduction occurs in amorphous thin films that does not occur in crystalline powders. This reduction was observed in RSD films deposited on glass and aluminum as well as titanium. Because it occurred within the first 50 regardless of oxide thickness, it therefore is unrelated to the substrate. Most probably it results from the amorphous nature of the thin films and points to weaker bonds between Ti and O atoms which allow easier preferential sputtering of O atoms, in accordance with the predictions of Kelly's proposed model [23]. Such preferential sputtering would not be expected in the crystalline polymorphs, particularly rutile, which have a higher heat of formation.[24]

Altogether, these results seem to confirm the opinion that amorphous films are inherently less stable thermodynamically than their crystalline forms.[25] It is tempting to project the decreased stability of amorphous oxides to a humid environment, and conclude that, at least for titanium, it will lead to degradation of adhesive bonds. We have identified four possible mechanisms leading to degradation: dissolution, surface migration and solid-state crystallization of the oxide, and diffusion of various species through the oxide leading to micro-corrosion of the base metal.

---

23 R. Kelly, Surf. Sci. 100, 85 (1980).

24 F.D. Rossini, D.D. Wagman, W.H. Evans, S. Levine, and I. Jaffe, Selected Values of Chemical Thermodynamics Properties (National Bureau of Standards, Washington, DC, 1952).

In general, we would hesitate to use AES peak-to-peak ratios to reliably indicate film stoichiometry in amorphous oxide films. However, in this case, the ratios observed at steady state were so much lower than those of TiO_2 crystals, that they strongly suggested existence of a non-stoichiometric, oxygen-poor oxide. Moreover, in addition to the probable reduction, the precipitous decrease in the O to Ti ratio close to the surface may be real and indicative of an average stoichiometry gradient. In RSD and anodized films, non-stoichiometry may occur if the film contains various oxide phases or O species, such as in rf-sputtered SiO_2,[26] or if the amorphous film is composed of perfectly stoichiometric clusters bound by oxygen-poor channels.[27] It is commonly assumed that amorphous oxide films contain oxygen vacancies and these were recently used to explain some electrical properties.[28] Defects in general and oxygen vacancies in particular may be very important factors in the corrosion protection behavior of oxide films, a topic that has received very little attention to date. On titanium they may enhance diffusion through an anodic film and contribute to a corrosion process whereby first TiO and then anatase are formed both in an anodic layer and on a "clean" Ti substrate. The exact mechanism of corrosion and especially the locus of reaction (substrate-film interface or film-solution interface) and the diffusing species remain to be determined. A kinetic

---

26 J.W. Coburn and E. Kay, Appl. Phys. Lett, 18, 435 (1971).
27 J.J. Hauser, G.A. Pasteur, A. Standinger, and R.S. Hutton, J. Non-Cryst. Solids, 46, 59 (1981).
28 J.W. Schultze, U. Stimming, and J. Weise, Ber. Bunsenges, Phys. Chem. 86, 276 (1982).

study of the corrosion, preferably on pure Ti, is needed to clarify these points.

Since this work was not intended as a corrosion study of titanium, we did not use the usual electrochemical and weight measurement methods. However, AES profiling proved very useful in establishing the existence of a corrosion process on supposedly passivated Ti, under conditions (pure water, $T < 100°C$) where no corrosion is expected. This technique should be developed further. Although it has disadvantages, e.g., the measurement is done on selected samples after corrosion for various times, they are compensated for by: great sensitivity to oxide mass changes on the surface, good depth resolution, and the possibility of extracting information about chemical phases and even crystallinity. We believe that refinements will make it an excellent tool for kinetic studies of corrosion.

Finally, this study suggests that formation of a stable (i.e., crystalline), microrough, thick oxide is necessary for a strong and durable bond. A layer of anatase crystallites protruding from the surface, such as that obtained by immersing a clean Ti-6Al-4V surface in hot water, is likely to provide good adhesion for epoxy. Amorphous oxides that have a highly defective structure and are probably non-stoichiometric will be unstable in the long term and will contribute to bond degradation at high temperatures even in dry atmospheres. Future work should emphasize both practical methods of direct preparation of crystalline oxides, and basic studies of the defect structures of amorphous films and their effect on such processes as diffusion, crystallization, and base metal corrosion.

VI. REFERENCES

1. B.M. Ditchek, K.R. Breen, T.S. Sun, J.D. Venables, and S.R. Brown, in Proc. 12th Natl. SAMPE Tech. Conf. (Seattle, WA, 1980), p. 882.

2. B.M. Ditchek, K.R. Breen, T.S. Sun and J.D. Venables, in Proc. 25th Natl. SAMPE Symp. (San Diego, CA, 1980), p. 13.

3. M. Natan, J.D. Venables, and K.R. Breen, in Proc. 27th Natl. SAMPE Symp. (San Diego, CA, 1982), p. 178.

4. M. Natan and J.D. Venables, submitted to J. of Adhesion.

5. A.A. Roche, J.S. Solomon, and W.L. Baun, Appl. Surf. Sci. 7, 83, (1981).

6. J.M. Abd El Kader, F.M. Abd El Kader, H.A. El Shayeb, and M.G.A. Khedr, Br. Corros. J. 16, 111 (1981).

7. F. Dalard, C. Montella, and J. Gandon, Surf. Technol. 8, 203 (1979).

8. G. Blondeau, M. Froelicher, M. Forment, and A. Hugot-LeGoff, in Proc. 7th Int. Vac. Congr. and 3rd Int. Conf. Solid Surf. (Vienna, 1977), p. 1789.

9. K.W. Allen, H.S. Alsalim, and W.C. Wake, J. Adhes. 6, 153 (1974).

10. A. Polity, G. Jouve, and P. Lacombe, J. Less-Com. Met. 56, 263 (1977).

11. J.D. Venables, D.K. McNamara, J.M. Chen, B.M. Ditchek, T.I. Morgenthaler, and T.S. Sun, Proc. 12th National SAMPE Conf. (Seattle, WA, 1980), p. 909

12. M. Natan, K.R. Breen, and J.D. Venables, MML TR 81-42(c), Martin Marietta Laboratories, Baltimore, MD, Report to Navairsyscom, September 1981.

13. J.T. Grant, T.W. Haas, and J.E. Houston, J. Vac. Sci. Technol. 11, 227 (1974).

14. J. Gandon and J.C. Joud, J. Less-Com. Met. 69, 277 (1980).

15. J.S. Solomon and W.L. Baun, Surf. Sci. 51, 228 (1975).

16. C.N.R. Rao and D.D. Sarma, Phys. Rev. B 25, 2927 (1982).

17. S. Thomas, Surf. Sci. 55, 756 (1976).

18. M.L. Knotek and J.E. Houston, Phys. Rev. B 15, 4580 (1977).

19. H.J. Mathieu, J.B. Mathieu, D.E. McClure, and D. Landolt, J. Vac. Sci. Technol. 14, 1023 (1977).

20. M.R. Armstrong and R.K. Quinn, Surf. Sci. 67, 451 (1977).

21. A.C. Fraker and A.W. Ruff, Corrosion Sci, 11, 763 (1971).

22. M. Shiojiri, J. Phys. Soc. Japan, 21, 335 (1966).

23. R. Kelly, Surf. Sci. 100, 85 (1980).

24. F.D. Rossini, D.D. Wagman, W.H. Evans, S. Levine, and I. Jaffe, Selected Values of Chemical Thermodynamics Properties (National Bureau of Standards, Washington, DC, 1952).

25. K.H. Behrndt, J. Vac. Sci. Technol. 7, 385 (1970).

26. J.W. Coburn and E. Kay, Appl. Phys. Lett, 18, 435 (1971).

27. J.J. Hauser, G.A. Pasteur, A. Standinger, and R.S. Hutton, J. Non-Cryst. Solids, 46, 59 (1981).

28. J.W. Schultze, U. Stimming, and J. Weise, Ber. Bunsenges Phys. Chem. 86, 276 (1982).

DISTRIBUTION LIST

ADDRESSEE	COPIES
Commander Naval Air Systems Command Washington, DC 20361 ATTN: Code AIR-5304	4
Commander Naval Air Systems Command Washington, DC 20361 ATTN: Code AIR-00D4	8
Commander Naval Air Systems Command Washington, DC 20361 ATTN: Code AIR-320A	1
Commander Naval Surface Weapons Center White Oak, Silver Spring, MD 20910 ATTN: Dr. Joseph Augl (Code 234)	1
Air Force Materials Laboratory Wright-Patterson AFB, OH 45433 ATTN: Codes: MBC MXE LN LAE LT LAM	6
Director Plastics Technical Evaluation Center U.S. Army Armament R&D Command Dover, NJ 07801	1
Hercules Incorporated Magna, UT 84044 ATTN: Mr. E. G. Crossland	1
TRW One Space Park Rodundo Beach, CA 90278 ATTN: R. W. Vaughan	1
University of Maryland College Park, MD 20742 ATTN: Dr. W. J. Bailey	1
Naval Research Laboratory Washington, DC 20375 ATTN: Chemistry Div. (Code 6170)	1
North American Aviation Rockwell International Columbus Division 4300 E. Fifth Ave. Columbus, OH 43216	1

DISTRIBUTION LIST (Cont'd)

ADDRESSEE	COPIES
Commanding Officer Naval Air Development Center Warminster, PA 18974 ATTN: Aero Materials Lab (Code 606)	1
Northrup Corporation 1001 E. Broadway Hawthorne, CA 90250 ATTN: Technical Library	1
Lockheed-California Co. Dept. 74-54, Bldg. 63 Box 551 Burbank, CA 91503 ATTN: Mr. J. H. Wooley	1
Naval Research Laboratory Washington, DC 20350 ATTN: Code 6120 (1 copy) Code 8433 (1 copy)	2
The Boeing Co. Aerospace Division P. O. Box 3707 Seattle, WA 98124 ATTN: Library	1
Office of Naval Research Washington, DC 20361 ATTN: Code 471	1
NASA Headquarters 600 Independence Ave., SW Washington, DC 20546	1
Battelle Columbus Laboratories 505 King Avenue Columbus, OH 43201	1
Commander Naval Material Command Hdqtrs Washington, DC 20361 ATTN: Code MAT 04H	1
Lockheed Missiles and Space Center Sunnyvale, CA 94088 ATTN: Mr. Clayton May	1
Materials Engineering Laboratory U.S. Army Armament R&D Command Dover, NJ 07801 ATTN Mr. R. F. Wegman	1

DISTRIBUTION LIST (Cont'd)

National Academy of Science — 1
2101 Constitution Ave., NW
Washington, DC 20418
ATTN; Dr. R. S. Shane, NMAB

Stanford Research Institute — 2
333 Ravenswood Ave
Menlo Park, CA 94025
ATTN: Mr. M. Maximovich (1 copy)
Technical Library (1 copy)

Commander, Naval Ship Engineering Center — 1
National Center #2, Rm 5E52
Washington, DC 20361
ATTN: Mr. John Alfers

Commanding Officer — 1
Naval Air Rework Facility, NAS
Norfolk, VA 23511
ATTN: Mr. H. Sommerflek, Code 343

Commanding Officer — 1
Naval Air Rework Facility, NAS
Jacksonville, FL 32212
ATTN: Code 343

Commanding Officer — 1
Naval Air Rework Facility
Marine Corps Air Station
Cherry Pt., NC 28533
ATTN: Mr. F. Latham, Code 343

Commanding Officer — 1
Naval Air Rework Facility, NAS
North Island, San Diego, CA 92123
ATTN: Ms Carol Duesler, Code 343

Commanding Officer — 1
Naval Air Rework Facility, NAS
Alameda, CA 94501
ATTN. Mr. Norman Amdur, Code 343

Commanding Officer — 1
Naval Air Rework Facility, NAS
Pensacola, FL 32508
ATTN: Mr. Faoro, Code 343

McDonnell-Douglas Airplane Co. — 1
P. O. Box 516
St. Louis, MO 63166
ATTN: Dr. J. Carpenter (Materials)

Grumman Aerospace Corp — 1
Bethpage, LI, NY 11714
ATTN: Technical Library

Commander — 1
Naval Air Systems Command, Code AIR-8031B2
Washington DC 20361